Electronic and geometrical structure of Mn_{13} anions, cations, and neutrals

G. L. Gutsev,[1,a)] M. D. Mochena,[1] Charles W. Bauschlicher, Jr.,[2] W.-J. Zheng,[3] O. C. Thomas,[3] and Kit H. Bowen[3,a)]
[1]*Department of Physics, Florida A&M University, Tallahassee, Florida 32307, USA*
[2]*Mail Stop 230-3, NASA Ames Research Center, Moffett Field, California 94035, USA*
[3]*Department of Chemistry and Department of Materials Science, Johns Hopkins University, Baltimore, Maryland 21218, USA*

(Received 15 May 2008; accepted 17 June 2008; published online 25 July 2008)

We have computed the electronic and geometrical structures of thirteen atom manganese clusters in all three charge states, Mn_{13}^-, Mn_{13}^+, and Mn_{13} by using density functional theory with the generalized gradient approximation. Our results for Mn_{13}^- are compared with our anion photoelectron spectrum of Mn_{13}^-, published in this paper. Our results for Mn_{13}^+ are compared with the previously published photoionization results of Knickelbein [J. Chem. Phys. **106**, 9810 (1997)]. There is a good agreement between theoretical and experimental values of ionization and electron attachment energies. © *2008 American Institute of Physics*. [DOI: 10.1063/1.2956494]

I. INTRODUCTION

Manganese clusters, Mn_n, are intriguing species[1,2] whose ground states undergo a ferro- to ferrimagnetic transition[3,4] as the number of atoms, n, increases. The size of the cluster for which the transition occurs depends on the charge and equals 5, 6, and 3 in the neutral,[3,4] anionic,[5] and cationic[5] series, respectively. In addition, Mn_5 and Mn_6 were found to possess noncollinear local magnetic moments on the atoms.[6–9] Noncollinear magnetic structure studies have been extended to larger clusters (up to Mn_8 in Ref. 10, up to Mn_{19} in Ref. 11, and up to Mn_{55} at the bulk-type geometries in Ref. 12).

On the experimental side, anion photoelectron spectra[13] were obtained for Mn_n^-, $n=3-8$. They showed an increase in electron detachment energies with increasing n. Also, ionization energies were previously measured[14] for Mn_n clusters in the range of $7 \leqslant n \leqslant 64$. While a generally monotonic decrease in ionization energies (from 5.44 to 4.37 eV) was observed, deviations from this trend were seen at the smallest sizes, as well as at $n=13$ and 19. Stern–Gerlach experiments were performed for Mn_n clusters in the ranges of $11 \leqslant n \leqslant 99$ (Ref. 15) and $5 \leqslant n \leqslant 22$.[16] The largest differences in the magnetic moment per atom of Mn_n, with respect to Mn_{n-1} and Mn_{n+1}, were observed at $n=13$ and 19. Furthermore, optical spectra were obtained[17] for the Mn_3^+ trimer, and dissociation energies were measured[18,19] for Mn_2^+ to Mn_7^+.

The ground state of neutral Mn_{13} was found[20] to possess an icosahedral geometrical structure, which is typical for several other $3d$-metal clusters M_{13} such as Sc_{13},[21] Ti_{13},[22] and Fe_{13}.[23] Mn_{13} icosahedrons are also found to be the building units in the bulk GaMn compounds.[24] The magnetic moment per atom obtained by Nayak *et al.*[20] is $2.54\mu_B$, while the experimental value, which was measured later, is $0.54 \pm 0.06\mu_B$.[16] Kawazoe *et al.*[25] confirmed that the ground state structure is icosahedral and obtained the magnetic moment of $0.23\mu_B$ per atom. Subsequent studies[26,27] arrived at the same structure, magnetic moment, and distributions of spin-up and spin-down excess electron density as those found by Kawazoe *et al.*[25]

Our present work combines an experimental anion photoelectron spectroscopy study of the Mn_{13}^- anion and a theoretical search for the lowest total energy isomers of Mn_{13}^- and Mn_{13}^+. Geometrical optimizations were performed over a wide range of the spin multiplicities using all-electron density functional theory with generalized gradient approximation and flexible basis sets. After discussing both the experimental and theoretical methods and procedures used in this work, we present our experimental data on Mn_{13}^- and then compare it, along with the previous data[12] on Mn_{13}^+, to our theoretical results, including geometrical structures and excess electron densities as well as the electron affinity (EA_{ad}) and the ionization potential (IP) of Mn_{13}.

II. EXPERIMENTAL METHODS

Anion photoelectron spectroscopy is conducted by crossing a beam of mass-selected negative ions with a fixed-frequency photon beam and energy analyzing the resultant photodetached electrons. The photodetachment process is governed by the energy-conserving relationship, $h\nu$=EBE +EKE, where $h\nu$ is the photon energy, EBE is the electron binding energy, and EKE is the electron kinetic energy. Briefly, our apparatus consists of an ion source, a linear time-of-flight mass analyzer (TOF-MS), a Nd:YAG photodetachment laser, and a magnetic bottle photoelectron spectrometer (MB-PES). The instrumental resolution of the MB-PES is ~35 meV at 1 eV EKE. The third (355 nm, 3.49 eV) harmonic of a Nd:YAG was used to photodetach electrons from the cluster anions of interest. Photoelectron spectra were calibrated against the well-known transitions of the Cu^- anion. Manganese cluster anions were generated in a laser vaporization source in which a rotating, translating manganese rod was irradiated with 532 nm (2.33 eV) pulses from a second Nd:YAG laser, while nearly simultaneously bursts of

[a)]Authors to whom correspondence should be addressed. Electronic mail: gennady.gutsev@famu.edu; kbowen@jbu.edu.

helium gas (~3 atm) from the rear of the source were passing over the manganese rod. The rapidly expanding gas cooled the resulting plasma and generated the manganese cluster anions.

III. COMPUTATIONAL METHODS AND PROCEDURES

Computations were performed using the GAUSSIAN 03 (Ref. 28) programs system. The primary basis set used is 6-311+G^*,[29] (15*s*11*p*6*d*1*f*)/[10*s*7*p*4*d*1*f*], while the 6-311 +$G(2d)$ basis set, (15*s*11*p*6*d*2*f*)/[10*s*7*p*4*d*2*f*], was used for estimating the dependence of the results obtained on *f*-function extensions. As in our previous work on Mn and iron clusters[5,30] we choose the BPW91 method, where the exchange-correlation functional is comprised of the Becke's exchange[31] and Perdew–Wang's correlation.[32] This preference is based on the results of our calibration calculations[33] on the Fe_4 cluster performed by six different DFT methods. While providing similar spectroscopic constants as the other methods, the BPW91 method was found to be less sensitive to a numerical integration grid used in computations of the exchange and correlation contributions. This allows us to use less computationally demanding integration grids. A comprehensive comparison of semilocal and hybrid density functionals is beyond the scope of this work, but may be found elsewhere.[34]

We assume a collinear treatment of the magnetic structure. According to the most recent study,[11] the lowest energy collinear structure of Mn_{13} with the spin multiplicity of 4 is degenerate in total energy with the lowest non-collinear structure, which justifies our collinear computations.

We performed searches of the lowest energy states whose geometrical configurations possessed icosahedron and nonicosahedron topologies. The Mn_{13} nonicosahedron geometries depend strongly on the spin multiplicity of the electronic state and generally are very similar to the geometries of the lowest excited states found[23] for Fe_{13}. Some other Mn_{13} states were considered previously,[26] but no state was closer than 0.89 eV to the icosahedral ground state.

A search for the lowest energy ferrimagnetic state is rather complicated,[35] because there are a larger number of possible orientations of the excess spin-up and spin-down densities. For ferrimagnetic trial guesses, we used spin-up and spin-down combinations produced in computations on singly and doubly charged ferrimagnetic Mn_{13} and Fe_{13} ions. We also created Mn_{13} guess vectors by superimposing Mn atom vectors, where the spin-up and spin-down occupation for each atom in the cluster was set by hand. Each geometry optimization was followed by an analytical second derivatives calculation of the harmonic vibrational frequencies in order to confirm that the optimized geometry corresponds to a minimum. The total energies obtained were used to evaluate the adiabatic electron attachment (electron affinity) and detachment (ionization potential) energies of Mn_{13}. The zero-point vibrational energies are similar for ground-state Mn_{13} (0.324 eV), Mn_{13}^- (0.319 eV), and Mn_{13}^+ (0.322 eV) and were neglected in these calculations. Excess electron spin densities on atoms were obtained using natural atomic orbital populations (NAO) as implemented in the NBO suite.[36]

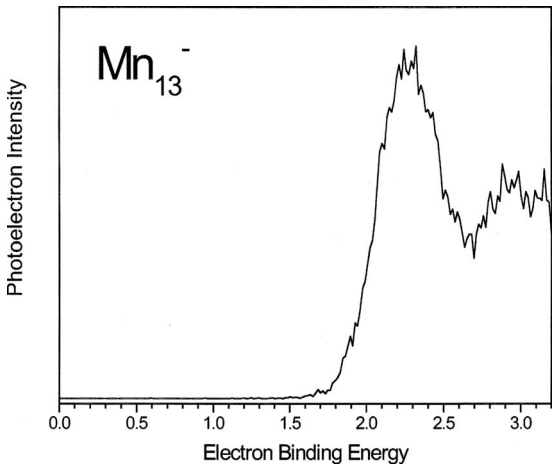

FIG. 1. Photoelectron spectrum of Mn_{13}^- measured with 3.49 eV photons.

VI. RESULTS AND DISCUSSION

A. Photoelectron spectrum of Mn_{13}^-

Our anion photoelectron spectrum of Mn_{13}^- measured with 3.49 eV photons is shown in Fig. 1. Its average vertical detachment energy, VDE, is 2.2 ± 0.1 eV. The VDE is the EBE of the maximum in the lowest EBE spectral band. It is the EBE of the maximal Franck–Condon overlap in the photodetachment transition between the ground state of the Mn_{13}^- anion and the ground state of its corresponding Mn_{13} neutral. The adiabatic electron affinity, EA_{ad}, is estimated to be 1.9 ± 0.1 eV. The EA_{ad} value is taken from the fast rising portion of the low EBE side of the lowest EBE band just above threshold. The EA_{ad} is defined as the energy difference between the lowest vibrational level of the anion's ground electronic state and the lowest vibrational level of the ground electronic state of its neutral counterpart. The second band centered around ~2.9 eV is the result of a photodetachment transition from the ground state of the Mn_{13}^- anion to an excited state of the Mn_{13} neutral.

B. Geometrical configurations and excess spin densities

The lowest total energy configurations of neutral Mn_{13} with different excess spin density patterns are presented in Fig. 2. As is seen, there are a large number of states within 0.3 eV of the ground state. To aid in an understanding of the origin of the states, the atoms with an excess spin up density are shaded dark, while those with an excess spin down density are shaded light. It is interesting to note that the lowest energy states may arise from different distributions of the spin density patterns. For example, while the lowest states with $2S+1=4$ and $2S+1=6$ have the same spin patterns, the lowest $2S+1=2$ state has a different spin pattern, and it is the first excited doublet state that has the same pattern as the lowest states with $2S+1=4$ and $2S+1=6$.

The spin multiplicity and excess spin density pattern obtained for the ground state of Mn_{13} is similar to that found by Kawazoe *et al.*[25] and in subsequent work.[26,27] The magnetic moment per atom is computed as twice the total spin divided by the number of atoms and is $0.23\mu_B$ in the Mn_{13} ground

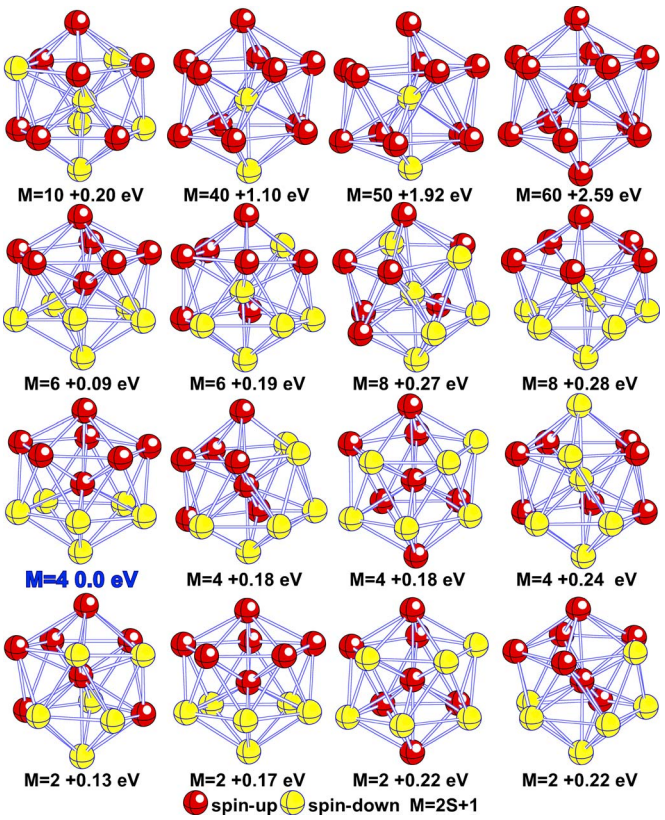

FIG. 2. (Color online) Excess spin density patterns in the lowest energy states of different spin multiplicities of neutral Mn_{13}. Energy separations are given with respect to the ground state total energy. The atoms with excess spin up density are shaded dark, while those with excess spin down density are shaded light.

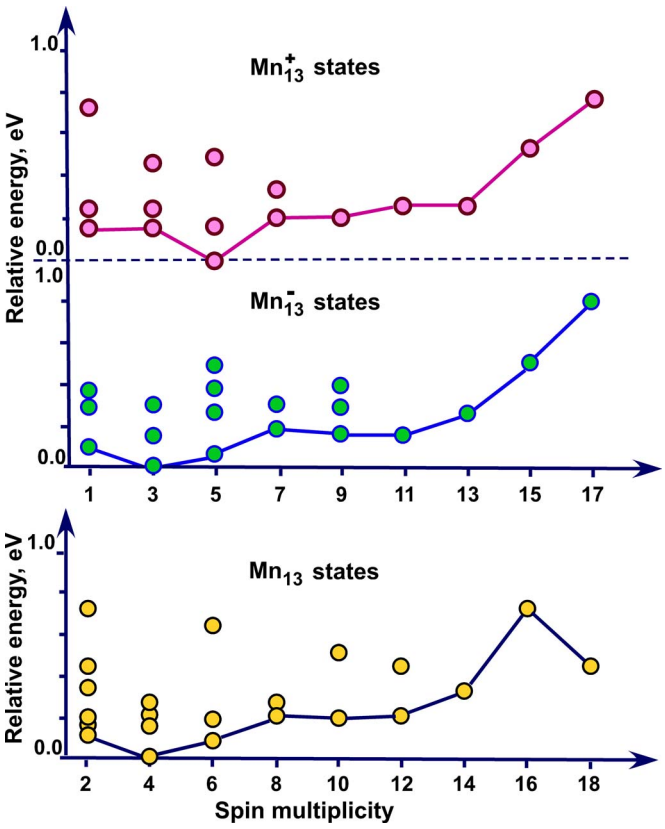

FIG. 3. (Color online) Total energy shifts of the Mn_{13}^- and Mn_{13}^+ isomers with different spin multiplicity given with respect to the corresponding ground states.

state, which is substantially smaller than the experimental value of $0.54 \pm 0.06 \mu_B$.[16] This discrepancy may be related to omitting the orbital moment contribution since the total magnetic moment $M=2S+L$. According to the results of computations performed[37] for Ni_n clusters using a model Hamiltonian, the orbital moment contribution may represent 20%–40% of the total magnetization and is therefore important for comparing theory and experiment. On the other hand, the neutral state with $2S+1=6$ is higher than the ground state by 0.087 eV only. If this state was involved in Knickelbein's experiment[16] then the discrepancy is significantly reduced.

The search for the lowest energy states of Mn_{13}^- and Mn_{13}^+ was performed using the neutral electronic densities of states presented in Fig. 2 as initial guesses, as well as using the converged electronic densities of the anion in optimizations of the cation and vice versa. The relative energies obtained in all three series are presented in Fig. 3. As is seen, there are a number of states that are close in total energy with the same or different spin multiplicities. The lowest energy states found for the anion and cation have the spin multiplicity of 3 and 5, respectively, and these states possess the same excess spin density pattern as the neutral ground state. The same spin multiplicity of Mn_{13}^- was obtained in the recent pseudopotential calculations.[38]

The detailed structures of the Mn_{13}, Mn_{13}^-, and Mn_{13}^+ ground states are presented in Fig. 4. The ground states of both neutral and anion have C_{5v} symmetry while the cation ground state has C_1 symmetry. In order to gain insight into asymmetry of spin-up (α) and spin-down (β) excess spin density distributions in the neutral ground state, consider the results of the NAO population analysis presented in Table I. As is seen, the total effective atomic electron configurations are close to $(3d^6 4s^1)$, except for the central atom with $(3d^{7.5} 4s^1)$. The central atom population probably suffers from some population artifacts due to the large overlap population; therefore, we believe all atoms have a $(3d^6 4s^1)$ occupation. In the atomic case, the promotion Mn $^6S(3d^5(^6S)4s^2) \rightarrow$ Mn $^6D(3d^6(^5D)4s^1)$ requires[39] 2.15 eV and is the largest among the $3d$ atoms.

An inspection of Fig. 4 shows that the excess spin on the central atom is significantly smaller then those on the surface, suggesting that the spin coupling of the d shell has changed from ^5D to allow additional bonding with the surface atoms. An inspection of Morse[39] shows that such a spin recoupling of the $3d$ shell requires significant energy, but since only one atom is involved, it appears to be favorable.

Attachment of an extra electron influences mostly the apex atoms whose distances from the central atom are affected more than those of the ring atoms. The excess spin density of the top apex atom decreases by $0.5e^-$, while the excess spin-down densities of the bottom ring atoms uniformly decreases by $0.1e^-$ (see Fig. 4). This results in the decrease of the total spin by one. The hole formed due to the electron detachment is delocalized over the cluster, mostly affecting the atoms with the spin-up excess spin density.

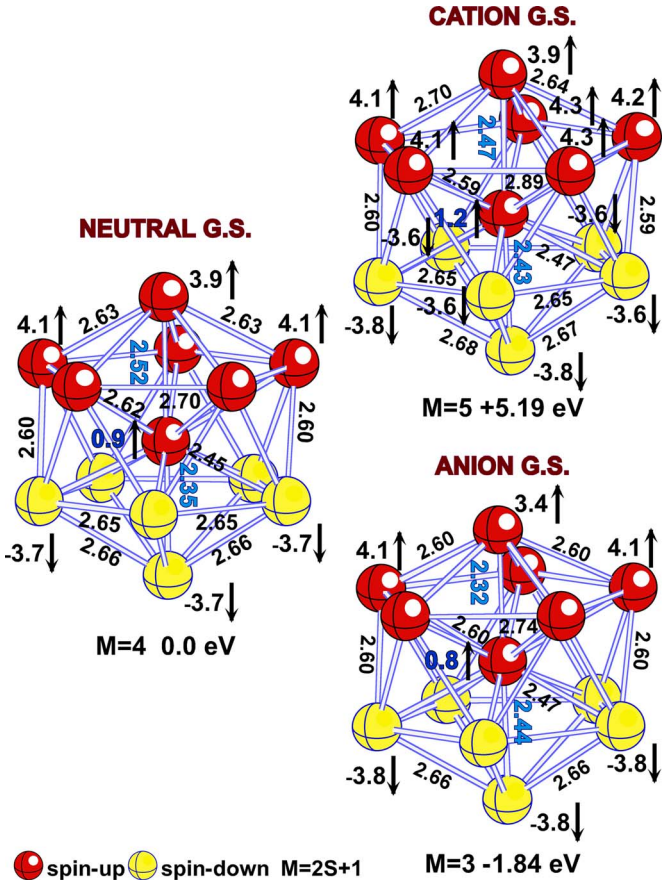

FIG. 4. (Color online) Geometrical configurations and excess spin densities of the ground-state Mn_{13}, Mn_{13}^-, and Mn_{13}^+ clusters. Bond lengths are in Å; excess spin densities are in electrons.

C. Electron detachment from Mn_{13}^- and ionization of Mn_{13}

Experimentally, ionization processes, whether from anions or neutrals, correspond to vertical processes. If one assumes that electron detachment and ionization are one-electron processes, then the final spin multiplicities will differ by ± 1 from the spin multiplicity of the initial states involved in the process. Using the 6-311+$G(2d)$ basis set, we calculated the EA_{ad}, VDE, and IP values of Mn_{13} and Mn_{13}^-. (EA_{ad} and IP values are properties of neutrals, while VDE is a property of anions.)

To calculate the adiabatic electron affinity of Mn_{13}, we computed the energy difference between the optimized anion geometry and the optimized neutral geometry. (This quantity could also be referred to as the adiabatic detachment energy of Mn_{13}^-.) The value of EA_{ad} that we computed was 1.84 eV, in close agreement with our experimentally determined value

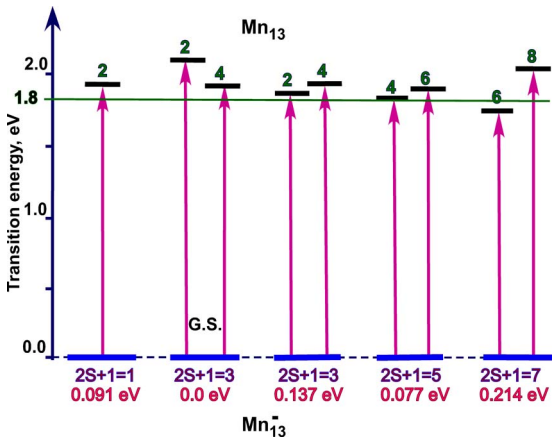

FIG. 5. (Color online) Energies of the vertical electron transition energies from the ground and four lowest energy excited states of the Mn_{13}^- anion. The energy shifts with respect to the ground state total energy are given below the spin multiplicities of the states involved.

of 1.9 eV. To calculate the VDE and other higher energy vertical transition energies of Mn_{13}^-, we computed the energy difference between the anion and neutral at the geometry of the Mn_{13}^- anion. Vertical transition energies from several lowest energy states of Mn_{13}^- are shown in Fig. 5. The Mn_{13}^- anion's ground state (labeled G.S.) has the spin multiplicity $2S+1=3$. The two lowest vertical electron transition energies are 1.92 and 2.12 eV (from $2S+1=3$ to $2S+1=4$ and from $2S+1=3$ to $2S+1=2$, respectively). These energies are rather close to each other and, along with Franck–Condon broadening, the width of the main band in the spectrum due to some degree of structural difference between the anion and its neutral, probably contribute to the width of the main band in the spectrum. Given this, agreement with the experimental VDE value of 2.2 eV is quite satisfactory.

Experimental ionization spectra obtained[14] for Mn_{13} shows two ionization energies, one at 4.82 ± 0.05 eV and the other one at 5.30 ± 0.05 eV. The experiment was interpreted in terms of the presence of two Mn_{13} isomers. Vertical transition energies from several of the lower energy states of neutral Mn_{13} are shown in Fig. 6. We found vertical electron transitions from the neutral Mn_{13} ground state, $2S+1=4$ to $2S+1=5$ of Mn_{13}^+ and to $2S+1=3$ of Mn_{13}^+ to be 5.26 and 5.39 eV, respectively. These are in good agreement the experimental value of 5.30 eV. Our computed value for the adiabatic ionization potential of Mn_{13} is 5.19 eV. In order to find an isomer that can be responsible for the value of 4.82 eV, we computed the vertical ionization energies for several excited states of Mn_{13}, including icosahedral and nonicosahedral isomers. The results of our computations for

TABLE I. NAO effective electronic configurations obtained for five types of atoms in the ground state of Mn_{13}.

Atoms	Total	Spin up	Spin down	Excess
Central	$3d^{7.53}4s^{0.97}4p^{0.15}$	$3d^{4.24}4s^{0.48}4p^{0.07}$	$3d^{3.29}4s^{0.49}4p^{0.08}$	0.9
Ring spin up	$3d^{5.86}4s^{0.93}4p^{0.07}$	$3d^{4.85}4s^{0.57}4p^{0.05}$	$3d^{1.01}4s^{0.35}4p^{0.02}$	4.1
Apex spin up	$3d^{6.05}4s^{0.80}4p^{0.08}$	$3d^{4.92}4s^{0.46}4p^{0.05}$	$3d^{1.13}4s^{0.33}4p^{0.03}$	3.9
Ring spin down	$3d^{5.94}4s^{0.86}4p^{0.05}$	$3d^{1.13}4s^{0.41}4p^{0.02}$	$3d^{4.80}4s^{0.44}4p^{0.04}$	−3.7
Apex spin down	$3d^{6.08}4s^{0.87}4p^{0.06}$	$3d^{1.24}4s^{0.39}4p^{0.03}$	$3d^{4.85}4s^{0.47}4p^{0.03}$	−3.7

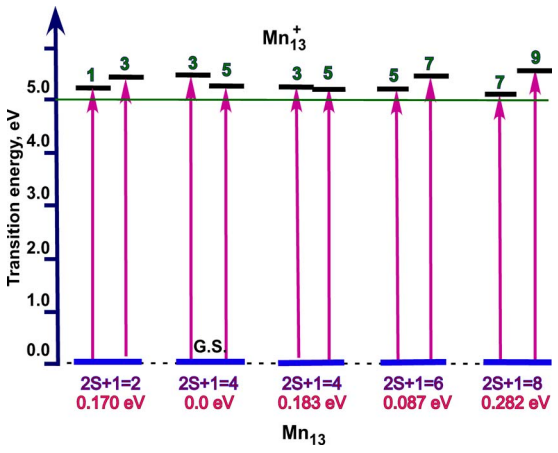

FIG. 6. (Color online) Energies of the vertical electron ionization energies from the ground and four lowest energy excited states of neutral Mn_{13}.

icosahedral isomers are presented in Fig. 6. The lowest ionization energy of 5.08 eV is found for the $2S+1=8$ state, which is 0.28 eV above the ground state. The vertical IPs from nonicosahedral isomers are also found around 5.30 eV. Therefore, a further effort is required to find an isomer responsible for the lower energy transition in the experimental ionization spectra.

V. CONCLUDING REMARKS

The results of the present Mn_{13} calculations are consistent with previous work for the spin multiplicity and overall distribution of spin up and spin down excess spin densities. As found in previous work, our magnetic moment per atom is $0.23\mu_B$, which is substantially smaller than the experimental value of $0.54\pm0.06\mu_B$.[16] Our measured vertical detachment energy, VDE, is 2.2 ± 0.1 eV and the adiabatic electron affinity is estimated to be 1.9 ± 0.1 eV. Our computed results are in good agreement with experiment giving support to the determination of both the ground state of the neutral and anion. Our computed IP is in good agreement with the larger experimental value of Knickelbein, but our results give no insight in the smaller experimental IP, which was interpreted as arising from an excited Mn_{13} isomer.

ACKNOWLEDGMENTS

G.L.G. thanks the Army MDA (Grant No. HQ0006-07-C-0016) for supporting the theoretical part of this work. K.H.B. thanks the Division of Materials Sciences and Engineering, Basic Energy Sciences, U.S. Department of Energy for support of the experimental part of this work under Grant No. DE-FG02-95ER45538.

[1] R. J. Van Zee, C. A. Baumann, S. V. Bhat, and W. Weltner, Jr., J. Chem. Phys. **76**, 5636 (1982).
[2] C. A. Baumann, R. J. Van Zee, S. V. Bhat, and W. Weltner, Jr., J. Chem. Phys. **78**, 190 (1983).
[3] P. Bobadova-Parvanova, K. A. Jackson, S. Srinivas, and M. Horoi, Phys. Rev. A **67**, 061202 (2003).
[4] N. O. Jones, S. N. Khanna, T. Baruah, and M. R. Pederson, Phys. Rev. B **70**, 045416 (2004).
[5] G. L. Gutsev, M. D. Mochena, and C. W. Bauschlicher, Jr., J. Phys. Chem. A **110**, 9758 (2006).
[6] T. Morisato, S. N. Khanna, and Y. Kawazoe, Phys. Rev. B **72**, 014435 (2005).
[7] R. C. Longo, E. G. Noya, and L. J. Gallego, J. Chem. Phys. **122**, 226102 (2005).
[8] R. C. Longo, E. G. Noya, and L. J. Gallego, Phys. Rev. B **72**, 174409 (2005).
[9] R. C. Longo, M. M. G. Alemany, J. Ferrer, A. Vega, and L. J. Gallego, J. Chem. Phys. **128**, 114315 (2008).
[10] J. Mejía-López, A. H. Romero, M. E. Garcia, and J. L. Morán-López, Phys. Rev. B **74**, 140405 (2006).
[11] M. Kabir, D. G. Kanhere, and A. Mookerjee, Phys. Rev. B **75**, 214433 (2007).
[12] Y. Xie and J. A. Blackman, Phys. Rev. B **73**, 214436 (2006).
[13] J. Jellinek, P. H. Acioli, J. Garciá-Rodeja, W. Zheng, O. C. Thomas, and K. H. Bowen, Jr., Phys. Rev. B **74**, 153401 (2006).
[14] G. M. Koretsky and M. B. Knickelbein, J. Chem. Phys. **106**, 9810 (1997).
[15] M. B. Knickelbein, Phys. Rev. Lett. **86**, 5255 (2001).
[16] M. B. Knickelbein, Phys. Rev. B **70**, 014424 (2004).
[17] A. Terasaki, T. M. Briere, M. Kulawik, S. Minemoto, K. Tono, A. Matsushita, and T. Kondow, J. Chem. Phys. **118**, 2180 (2003).
[18] A. Terasaki, S. Minemoto, and T. Kondow, J. Chem. Phys. **117**, 7520 (2002).
[19] K. Tono, A. Terasaki, T. Ohta, and T. Kondow, J. Chem. Phys. **123**, 174314 (2005).
[20] S. K. Nayak, M. Nooijen, and P. Jena, J. Phys. Chem. A **103**, 9853 (1999).
[21] H. K. Yuan, H. Chen, A. S. Ahmed, and J. F. Zhang, Phys. Rev. B **74**, 144434 (2006).
[22] M. Castro, S.-R. Liu, H.-J. Zhai, and L.-S. Wang, J. Chem. Phys. **118**, 2116 (2003).
[23] P. Bobadova-Parvanova, K. A. Jackson, S. Srinivas, and M. Horoi, Phys. Rev. B **66**, 195402 (2002).
[24] O. Gourdon and G. J. Miller, J. Solid State Chem. **173**, 137 (2003).
[25] T. M. Briere, M. H. F. Sluiter, V. Kumar, and Y. Kawazoe, Phys. Rev. B **66**, 064412 (2002).
[26] P. Bobadova-Parvanova, K. A. Jackson, S. Srinivas, and M. Horoi, J. Chem. Phys. **122**, 014310 (2005).
[27] M. Kabir, A. Mookerjee, and D. G. Kanhere, Phys. Rev. B **73**, 224439 (2006).
[28] M. J. Frisch *et al.*, GAUSSIAN 03, Revision D.01, Gaussian, Inc, Pittsburgh, PA, 2003.
[29] L. A. Curtiss, M. P. McGrath, J.-P. Blaudeau, N. E. Davis, R. C. Binning, Jr., and L. Radom, J. Chem. Phys. **103**, 6104 (1995).
[30] G. L. Gutsev, M. D. Mochena, E. Johnson, and C. W. Bauschlicher, Jr., J. Chem. Phys. **125**, 194312 (2006).
[31] A. D. Becke, Phys. Rev. A **38**, 3098 (1988).
[32] J. P. Perdew and Y. Wang, Phys. Rev. B **45**, 13244 (1992).
[33] G. L. Gutsev and C. W. Bauschlicher, Jr., J. Phys. Chem. A **107**, 7013 (2003).
[34] F. Furche and J. P. Perdew, J. Chem. Phys. **124**, 044103 (2006).
[35] P. Bobadova-Parvanova, K. A. Jackson, S. Srinivas, and M. Horoi, Phys. Rev. A **67**, 061202 (2003).
[36] A. E. Reed, L. A. Curtiss, and F. Weinhold, Chem. Rev. (Washington, D.C.) **88**, 899 (1988).
[37] R. A. Guirado-López, J. Dorantes-Dávila, and G. M. Pastor, Phys. Rev. Lett. **90**, 226402 (2003).
[38] J. Wang, J. Bai, J. Jellinek, and X. C. Zeng, J. Am. Chem. Soc. **129**, 4110 (2007).
[39] M. D. Morse, *Advances in Metal and Semiconductor Clusters* (JAI Press, Greenwich, CT, 1993), Vol. 1, pp. 83–121.